PHYSICS AND CHEMISTRY OF SOLID STATE
V. 25, No. 3 (2024) pp. 485-491
Section: Chemistry

DOI: 10.15330/pcss.25.3.485-491

Vasyl Stefanyk Precarpathian National University

ФІЗИКА І ХІМІЯ ТВЕРДОГО ТІЛА
Т. 25, № 3 (2024) С. 485-491
Хімічні науки

UDC: 546.882

ISSN 1729-4428 (Print)
ISSN 2309-8589 (Online)

L. Romaka[1], V.V. Romaka[2], Yu. Stadnyk[1], A. Horyn[1]

Experimental Study of Hf-Cu-Sn Ternary System at 870 K

[1]*Ivan Franko National University of Lviv, Lviv, Ukraine, lyubov.romaka@gmail.com*
[2]*Institute for Solid State Research, IFW-Dresden, Dresden, Germany, v.romaka@ifw-dresden.de*

Interaction of hafnium with copper and tin was studied at 870 K over the whole concentration range using X-ray diffractometry and scanning electron microscopy. At the temperature of investigation three ternary compounds are realized in the Hf-Cu-Sn system: HfCuSn (LiGaGe-type), $HfCu_5Sn_2$ ($HfCu_5Sn_2$-type), and Hf_5CuSn_3 (Hf_5CuSn_3-type). New $HfCu_5Sn_2$ ternary stannide crystallizes in the hexagonal space group $P6_3/mmc$ with cell parameters a = 0.42959(7) nm, c = 1.54165(4) nm. Electrical transport properties indicated metallic type of conductivity of the all studied ternary compounds. The DFT calculations were used to evaluate chemical bonding, elastic and physical properties of the ternary phases.

Keywords: intermetallics; phase diagrams; X-ray diffraction; crystal structure; electrical transport.

Received 10 January 2024; Accepted 19 August 2024.

Introduction

In the field of materials science many activities are devoted to the search of the new intermetallic alloys with promising physical properties. Among the intensively studied objects are Cu-Sn alloys which are characterized by high electrical and thermal conductivity, mechanical properties and good corrosion resistance [1, 2]. The Hf-Cu phases are basis for the preparation of amorphous alloys and thin films [3]. In many cases several factors play important role – temperature, composition, formation of atomic clusters, strong atomic bonding, structural defects. The previously studied Hf-Ni-Sn, Hf-Co-Sn and Hf-Ag-Sn [4-6] ternary systems indicate an influence of *d*-metals on the interaction of Hf and Sn with Ni, Co or Ag. Among them in the Hf-Ag-Sn system at 770 K no ternary phases were observed. In the case of equiatomic HfMSn compounds the type of 3*d*-metal leads to the different crystal structure – cubic MgAgAs-type (HfNiSn), hexagonal ZrNiAl-type (HfCoSn), and hexagonal LiGaGe-type (HfCuSn) [4, 5, 7]. The ternary phases with the Hf_5CuSn_3 structure type observed in the systems with of IVb group elements, copper and tin have been reported in Refs. [8].

In our paper we present the constructed phase diagram of the Hf-Cu-Sn ternary system at 870 K, structural, electrical and mechanical properties of the ternary phases. The crystal structure of the new $HfCu_5Sn_2$ compound covered by the DFT study is also presented.

I. Experimental

The alloys have been synthesized by direct arc melting of the constituent elements (Hf, Cu and Sn with nominal purity above 99.99 wt. %) under inert argon atmosphere (purified by Ti getter) on a water-cooled copper bottom. For better homogenization the alloys were re-melted twice. Samples were annealed for one month at 870 K in an evacuated silica tubes and then water-quenched. In the Cu-Sn system the most binaries are stable around ~870 K [9, 10] and the temperature 870 K for investigation of the Hf-Cu-Sn system over the whole concentration range was chosen.

Our attempt to use the higher annealing temperature (1070 K) was unsuccessful, particularly in the ternary part closed to the Cu-Sn system at Sn content more than 20 at. %. At 1070 K the ingots were completely melted in the ampoules in few hours. Some alloys were checked by DTA analysis (LINSEIS STA PT 1600 device, argon atmosphere). Samples were heated up to 1070 K, at a rate of 10 K/min. The weight losses during heating (TG) were

Table 1.

Crystallographic data of the binary phases in the Hf-Cu, Cu-Sn and Hf-Sn systems at 870 K

Phase	Pearson symbol	Space group	Structure type	Lattice parameters, nm		
				a	*b*	*c*
$Hf_{14}Cu_{51}$	hP68	*P6/m*	$Gd_{14}Ag_{41}$	1.1179(7)		0.81913(6)
Hf_3Cu_8	oP44	*Pnma*	Hf_3Cu_8	0.7812(3)	0.8103(5)	0.9948(5)
Hf_7Cu_{10}	oS68	*Cmce*	Zr_7Ni_{10}	1.2570(3)	0.9236(5)	0.9235(3)
Hf_2Cu	t16	*I4/mmm*	Zr_2Cu	0.3172(3)		1.1117(4)
$Cu_{0.85}Sn_{0.15}$	cI2	*Im-3m*	W	1.7973(8)		
Cu_3Sn (ht)	cF16	*Fm-3m*	BiF_3	0.6020(2)		
$Cu_{10}Sn_3$	hP26	$P6_3$	$Cu_{10}Sn_3$	0.7324(7)		0.7864(7)
Cu_3Sn (rt)	oP8	*Pmmn*	Cu_3Ti	0.4324(7)	0.5511(5)	0.4767(2)
$HfSn_2$	hP9	$P6_222$	$CrSi_2$	0.5470(2)		0.7599(4)
Hf_5Sn_3	hP16	$P6_3/mcm$	Mn_5Si_3	0.8333(2)		0.5694(3)

negligible (less than 0.3 %). Prepared samples were examined by X-ray diffraction and energy-dispersive X-ray spectroscopy (EDX) (Tescan Vega 3 LMU scanning microscope). For crystal structure study XRPD data were collected on a STOE STADI P diffractometer ($2\theta/\omega$-scan; Cu $K\alpha_1$ radiation, curved germanium (1 1 1) monochromator). Rietveld refinements were performed using the FullProf Suite program package [11].

Hardness measurements were performed by standard technique at a maximum load of 0.196 N. Seven indents was performed on each phase to verify the accuracy of the indentation data. Measurements of the temperature dependence of the electrical resistivity $\rho(T)$ was performed in the temperature range from 4.2 to 300 K by four-probe method using the helium cooler. Temperature dependence of electrical resistivity of the $HfCu_5Sn_2$ compound was measured in the temperature range 78 - 380 K.

The DFT calculations were carried out using the Elk v2.3.22 package [12] – an all-electron full-potential linearized augmented-plane wave (FP-LAPW) code with Perdew-Burke-Enzerhoff exchange-correlation functional in generalized gradient approximation (GGA) [13]. The *k*-point mesh grid was equal or higher than 12×12×12 *k*-points depending on the crystal structure of compound. Prior to the final total energy calculations the geometry of the initial structures (lattice vectors and atomic coordinates) was relaxed. The geometry optimization was carried out using calculation of the Hellman-Feynman forces with core and incomplete basis set corrections. The distribution of the densities of states (DOS) was calculated by trilinear method using 1000 *k*-point grid size for integrating functions in the Brillouin zone and 1000 energy points in the DOS plot. The interstitial DOS is included into the total DOS distribution, while the partial DOS for each atom type was obtained only within the volume of the appropriate muffin-tin sphere. The distributions of the charge density (ρ) and electron localization function (ϒ) were calculated by using 60×60×60 point grid and plotted by VESTA software package [14]. The 2nd order elastic properties of the ternary compounds with a relaxed geometry were calculated using FP-LAPW Exciting and ElaStic codes utilizing PBESol [15-17] exchange-correlation potential.

II. Results and discussion

To study the Hf-Cu-Sn system we analyzed the binary Hf-Cu, Hf-Sn and Cu-Sn system, which border the Hf-Cu-Sn ternary system [9, 10]. The crystallographic characteristics of the binary phases revealed at 870 K in the Hf-Cu, Cu-Sn and Hf-Sn systems are listed in Table 1.

To establish the chemical and phase composition the prepared Hf-Cu-Sn alloys were examined by X-ray powder diffraction and EPM analysis. Based on the obtained results the isothermal section of the Hf-Cu-Sn system was constructed at 870 K over the whole concentration range (Fig. 1). The phase composition and EPMA data for selected alloys are given in Table 2, microphotographs of some alloys are shown in Fig. 2.

Solubility of Sn in the $Hf_{14}Cu_{51}$ binary extends to ~17 at. % (a = 1.1179(7), c = 0.81913(6) nm for $Hf_{14}Cu_{51}$ binary, a = 1.1271(2), c = 0.8242(3) nm for $Hf_{20}Cu_{63}Sn_{17}$ sample). According to EPMA data the limit composition of the $Hf_{14}Cu_{51-x}Sn_x$ solid solution is $Hf_{22.02}Cu_{60.76}Sn_{17.22}$. In the Hf–{Co, Ni, Ag}–Sn systems [4-6] the compositions of the $Hf_5M_xSn_3$ solid solutions at x = 1.0 were considered as ternary phases with Hf_5CuSn_3-type. In the Hf-Cu-Sn system the XRPD analysis of the samples along Hf_5CuSn_3-Hf_5Sn_3 line showed the presence of the solid solution $Hf_5Cu_xSn_3$ up to the Hf_5CuSn_3 composition with variation of the lattice parameters from a = 0.8333(2), c = 0.5694(3) nm (for Hf_5Sn_3 binary) to a = 0.85101(4), c = 0.5815(3) nm (for Hf_5CuSn_3). According to EPMA data the limit composition ($Hf_{55.34}Cu_{10.75}Sn_{33.92}$) of the solid solution corresponds to the ternary Hf_5CuSn_3 phase. Additionally small homogeneity range (up to ~ 3 at. %) was observed for Hf_5Sn_3 binary toward to higher tin content.

Among the already known HfCuSn [7] and Hf_5CuSn_3 [8] ternary compounds the new ternary stannide $HfCu_5Sn_2$ was found. Crystallographic characteristics of the ternary stannides of the Hf-Cu-Sn system are listed in Table 3. All the ternary phases are formed up to ~40 at. % Sn.

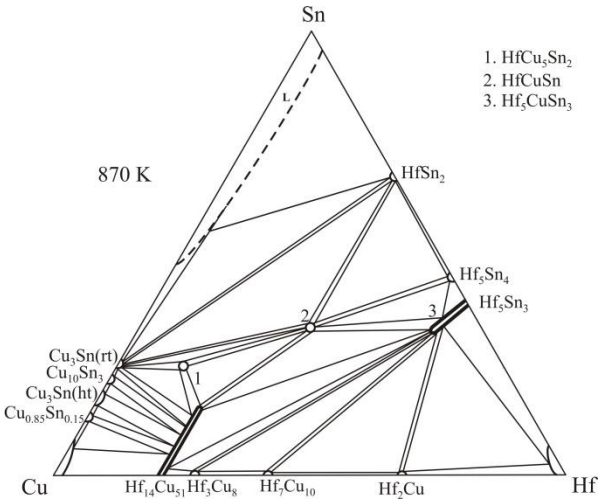

Fig. 1. Isothermal section of the Hf-Cu-Sn phase diagram at 870 K.

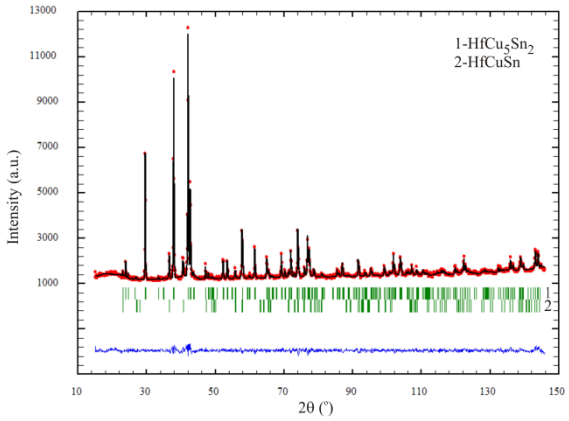

Fig. 3. The observed, calculated, and difference X-ray patterns of $Hf_{15}Cu_{60}Sn_{25}$ sample.

The new ternary phase $HfCu_5Sn_2$ was identified during the XRD phase analysis of the samples near ~$Hf_{15}Cu_{60}Sn_{25}$ composition. EPMA data revealed $Hf_{12.49}Cu_{62.16}Sn_{25.35}$ composition for this phase which corresponds to the $HfCu_5Sn_2$ stoichiometry. The powder pattern reflections of the $Hf_{15}Cu_{60}Sn_{25}$ sample were well indexed on the basis of a hexagonal lattice with cell parameters a = 0.42959(7) nm, c = 1.54165(4) nm (Fig. 3).

The structure of $HfCu_5Sn_2$ appeared to be very similar to the $HfCu_{2.73}Sb_{1.86}$ (space group $P6_3/mmc$) [18] and $YbFe_2Si_{4.5}$ (space group $P6_3/mmc$) [19] structure types with commensurate lattice parameters. For the refinements of the $HfCu_5Sn_2$ structure we used the mode l of the $YbFe_2Si_{4.5}$ type, where Hf atoms occupy the position 2*c* of Yb atoms, but unlike $YbFe_2Si_{4.5}$-type Cu atoms occupy the positions 4*e*, 4*f* and 2*b* of Si atoms and Sn atoms are located in position 4*f* of Fe atoms with their ordered distribution in the crystal structure. The refined atomic coordinates are listed in Table 4.

We have checked the $HfCu_5Sn_2$ compound using the differential thermal analysis and confirmed the limited temperature range of this phase. The DTA curve measured in the heating regime shows the thermal peak at about ~1020 K (Fig. 4) which can be associated with the decomposition of the $HfCu_5Sn_2$ phase.

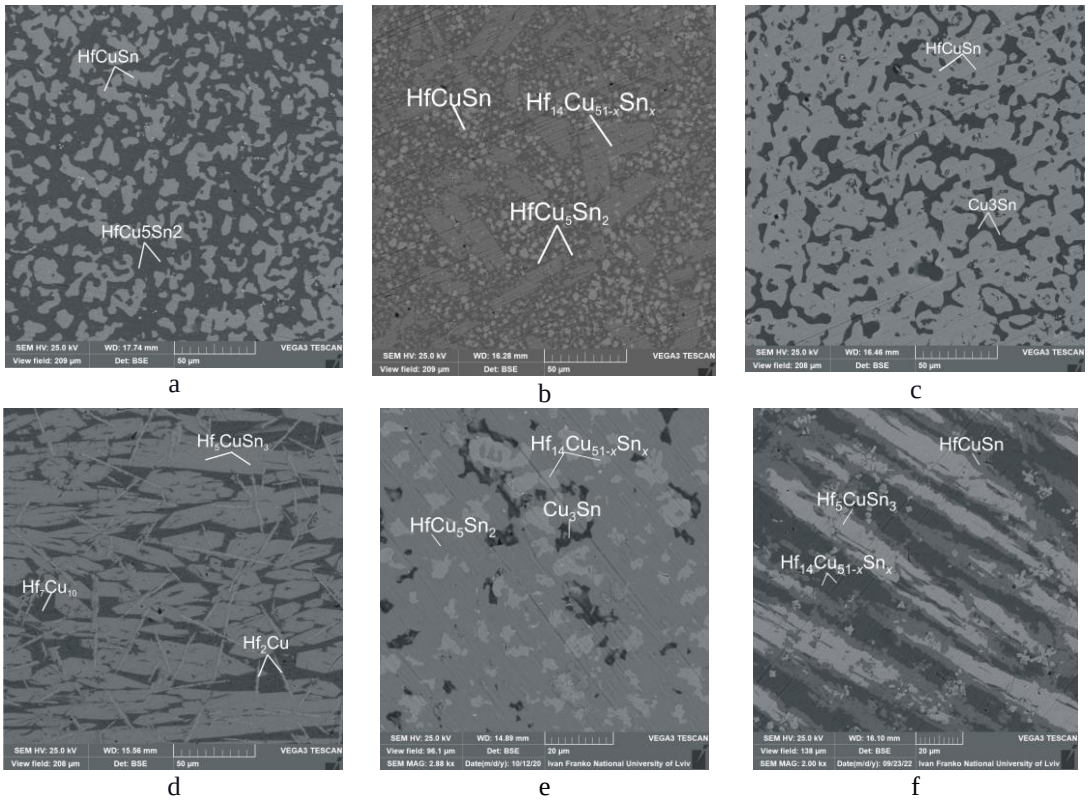

Fig. 2. Electron microphotographs of the alloys: a) $Hf_{22}Cu_{50}Sn_{28}$; b) $Hf_{20}Cu_{60}Sn_{20}$; c) $Hf_{20}Cu_{50}Sn_{30}$; d) $Hf_{55}Cu_{25}Sn_{20}$; e) $Hf_{13}Cu_{65}Sn_{22}$; f) $Hf_{40}Cu_{35}Sn_{25}$.

Table 2.

Phase composition and EPMA data for selected alloys in Hf-Cu-Sn system

Nominal composition, at. %	Phase	Structure type	Lattice parameters, nm			EPMA, at %		
			a	*b*	*c*	Hf	Cu	Sn
$Hf_{25}Cu_{60}Sn_5$	$Hf_{14}Cu_{51}$	$Gd_{14}Ag_{51}$	1.1179(7)		0.81913(6)	20.37	79.44	0.19
	Hf_5CuSn_3	Hf_5CuSn_3	0.8499(4)		0.5812(6)	55.49	11.02	33.49
$Hf_{30}Cu_{60}Sn_{10}$	$Hf_{14}Cu_{51-x}Sn_x$	$Gd_{14}Ag_{51}$	1.1238(3)		0.8236(6)	21.72	69.30	8.98
	Hf_5CuSn_3	Hf_5CuSn_3	0.8500(5)		0.5803(7)	55.66	10.79	33.55
$Hf_{10}Cu_{78}Sn_{12}$	Cu_3Sn (ht)	BiF_3	0.6118(7)					
	$Hf_{14}Cu_{51-x}Sn_x$	$Gd_{14}Ag_{51}$	1.1199(5)		0.8243(5)			
$Hf_{15}Cu_{70}Sn_{15}$	Cu_3Sn (rt)	Cu_3Ti	0.4326 (3)	0.5512(4)	0.4768(4)		73.93	26.07
	$Hf_{14}Cu_{51-x}Sn_x$	$Gd_{14}Ag_{51}$	1.1269(4)		0.8249(6)	21.33	62.75	15.92
$Hf_{45}Cu_{40}Sn_{15}$	Hf_3Cu_8	Hf_3Cu_8	0.7812(3)	0.8103(5)	0.9948(5)			
	Hf_5CuSn_3	Hf_5CuSn_3	0.8508(5)		0.5813(5)			
	Hf_7Cu_{10}	Zr_7Ni_{10}	1.2570(3)	0.9236(5)	0.9233(4)			
$Hf_{10}Cu_{74}Sn_{16}$	$Cu_{10}Sn_3$	$Cu_{10}Sn_3$	0.7324(7)		0.786(1)			
	$Hf_{14}Cu_{51-x}Sn_x$	$Gd_{14}Ag_{51}$	1.1266(2)		0.8242(2)			
$Hf_{70}Cu_{20}Sn_{10}$	$Hf_5Cu_xSn_3$	Hf_5CuSn_3	0.8479(4)		0.5783(4)	58.09	7.03	34.88
	Hf_2Cu	Zr_2Cu	0.3178(3)		1.1117(4)	67.09		32.91
	(Hf)	(Mg)	0.3183(3)		0.5054(4)	99.99		
$Hf_{55}Cu_{25}Sn_{20}$	Hf_7Cu_{10}	Zr_7Ni_{10}	1.2571(4)	0.9238(6)	0.9235(5)	40.80	57.87	1.33
	Hf_5CuSn_3	Hf_5CuSn_3	0.8479(5)		0.5794(7)	55.87	11.11	33.02
	Hf_2Cu	Zr_2Cu	0.3176(4)		1.1155(6)	69.67	30.33	
$Hf_{15}Cu_{60}Sn_{25}$	$HfCu_5Sn_2$	$HfCu_5Sn_2$	0.4296(7)		1.5416(8)	12.72	61.63	25.65
	HfCuSn	LiGaGe	0.4436(6)		0.6377(8)	33.56	33.45	32.99
$Hf_{12}Cu_{65}Sn_{23}$	Cu_3Sn	Cu_3Ti	0.4324(7)	0.5511(5)	0.4762(2)		74.46	25.54
	$HfCu_5Sn_2$	own	0.4260(6)		1.5415(4)	11.45	63.13	25.42
	$Hf_{14}Cu_{51-x}Sn_x$	LiGaGe	1.1272(4)		0.8243(6)	20.56	61.71	17.73
$Hf_{20}Cu_{50}Sn_{30}$	HfCuSn	LiGaGe	0.4436(3)		0.6388(7)	33.31	33.52	33.17
	Cu_3Sn	Cu_3Ti	0.4325(4)	0.5512(5)	0.4762(4)		74.79	25.21
$Hf_{57}Cu_{10}Sn_{33}$	Hf_5CuSn_3	Hf_5CuSn_3	0.85101(4)		0.5915(5)	56.23	10.75	33.02
$Hf_{25}Cu_{35}Sn_{40}$	HfCuSn	LiGaGe	0.4437(4)		0.6388(8)	33.28	33.61	33.11
	Cu_3Sn	Cu_3Ti	0.4320(5)	0.5494(8)	0.4747(6)		74.78	25.22
	$HfSn_2$	$CrSi_2$	0.5469(2)		0.7594(5)	32.89		67.11
$Hf_{15}Cu_{35}Sn_{50}$	(Sn)	Sn	0.5808(2)		0.3164(2)			100.0
	$HfSn_2$	$CrSi_2$	0.5470(2)		0.7598(5)	32.32		67.68
	Cu_3Sn	Cu_3Ti	0.4321(3)	0.5509(50	0.4742(4)		74.73	25.27
$Hf_{25}Cu_{25}Sn_{50}$	$HfSn_2$	$CrSi_2$	0.5470(3)		0.7594(8)	67.27		32.73
	HfCuSn	LiGaGe	0.4437(2)		0.6389(5)	33.61	31.71	34.68
	Cu_3Sn	Cu_3Ti	0.4325(3)	0.5509(5)	0.4742(4)		74.76	25.24

The Vickers hardness measurements (H_V) show close values for all three ternary compounds:
H_V(HfCuSn) = 3.46 GPa, H_V(Hf_5CuSn_3) = 3.75 GPa, and H_V($HfCu_5Sn_2$) = 4.15 GPa and are comparable with those from DFT calculations (Table 5). Experimental microhardness values for all studied ternary compounds are higher in comparison with elemental copper and hafnium (0.35 and 1.52-2.06 GPa, respectively) [20].

The temperature dependencies of electrical resistivity for two samples of the $Hf_5Cu_xSn_3$ solid solution: $Hf_5Cu_{0.3}Sn_3$ and Hf_5CuSn_3, are shown in Fig. 5,*a*. Increasing of resistivity with temperature indicates metallic type of conductivity of both phases. The resistivity data of both samples can be approximated by the Bloch–Grüneisen expression with values of the Debye temperature θ_D and residual resistivity ρ_0: 106.4 K,

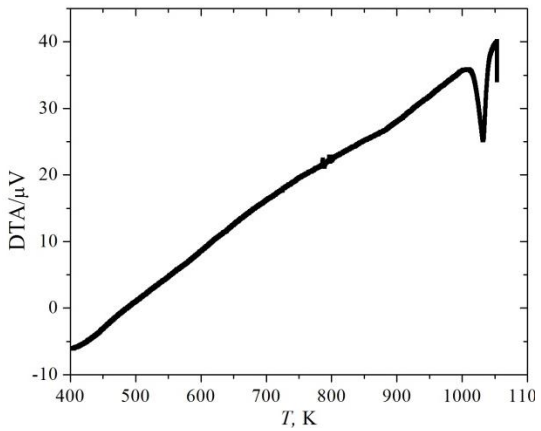

Fig. 4. DTA curve for the $HfCu_5Sn_2$ compound.

Table 3.

Crystallographic data for the ternary compounds in the Hf-Cu-Sn system

№	Compound	Structure type	Space group	Unit cell parameters, nm		
				a	*b*	*c*
1	$HfCu_5Sn_2$	$HfCu_5Sn_2$	$P6_3/mmc$	0.42959(7)		1.54165(4)
2	HfCuSn	LiGaGe	$P6_3mc$	0.44368(6)		0.6387(1)
3	Hf_5CuSn_3	Hf_5CuSn_3	$P6_3/mcm$	0.85101(4)		0.5815(5)

Table 4.

Atomic positional and isotropic displacement parameters for the $HfCu_5Sn_2$ compound (space group $P6_3/mmc$, $Z = 2$, $R_p = 0.0276$, $R_{wp} = 0.0355$, $R_{Bragg} = 0.092$)

Atom	Wyckoff position	*x*/*a*	*y*/*b*	*z*/*c*	B_{iso} 10^2 nm^2
Hf	2*c*	1/3	2/3	1/4	0.57(9)
Cu1	4*e*	0	0	0.1707(6)	0.88(4)
Cu2	4*f*	1/3	2/3	0.0541(7)	1.45(1)
Cu3	2*b*	0	0	1/2	1.12(2)
Sn	4*f*	1/3	2/3	0.6227(2)	0.69(1)

Table 5.

Second-order elastic constants, C_{ij} (GPa), bulk modulus, *B* (GPa), shear modulus, *G* (GPa), Young's modulus, *E* (GPa), Poisson's ratio, *v*, *B*/*G* ratio and Vickers hardness, H_V (GPa) of $HfCu_5Sn_2$, HfCuSn, and Hf_5CuSn_3

Compound	C_{11}	C_{12}	C_{13}	C_{33}	C_{44}	*B*	*G*	*E*	*v*	*B*/*G*	H_V
$HfCu_5Sn_2$	201.4	91.8	63.4	165.1	40.0	109.2	48.5	151.4	0.381	2.25	4.49
HfCuSn	201.2	83.0	83.5	190.1	69.2	121.3	61.8	151.5	0.316	1.96	7.14
Hf_5CuSn_3	217.0	93.6	65.5	242.2	57.7	125.1	63.9	214.6	0.381	1.96	7.37

38.3 μΩ·m (Hf_5CuSn_3), 144.6 K, 28.2 μΩ·m ($Hf_5Cu_{0.3}Sn_3$). Both studied samples are characterized by small values of electrical resistivity, however, for $Hf_5Cu_{0.3}Sn_3$ the resistivity with increasing of temperature changes more rapidly (from 28 μΩ·m to 64 μΩ·m at 300 K). The total change of resistivity of ordered phase Hf_5CuSn_3 is small – from 38 μΩ·m at 4 K to 47 μΩ·m at 300 K. The temperature dependence of electrical resistivity of the HfCuSn stannide is nearly linear in the interval 50 - 300 K (Fig. 5,*b*) and shows typical metallic behavior. The dependence was fitted by the Bloch–Grüneisen expression with $\theta_D = 89.0$ K and $\rho_0 = 22.6$ μΩ·m. The $HfCu_5Sn_2$ compound also shows metallic type of conductivity (Fig. 5,*c*) with Debye temperature 231.2 K and residual resistivity 14.8 μΩ·m.

In order to shed a light on the physical and elastic properties, bonding and crystal chemistry of HfCuSn, $HfCu_5Sn_2$, and Hf_5CuSn_3 intermetallics their electronic structure was modeled. The calculated heat of formation ΔH_f shows that Hf_5CuSn_3 is characterized by the highest value -348.2 meV/atom, while $HfCu_5Sn_2$ has the lowest value: -52.7 meV/atom. Ternary HfCuSn has intermediate value: -223.5 meV/atom. With the increasing of Hf content from 12.5 at.% in $HfCu_5Sn_2$, through 33.3 at.% in HfCuSn to 55.6 at.% in Hf_5CuSn_3 the heat of formation decreases almost linearly.

The calculated total distribution of electronic states (DOS) shows that all investigated ternary stannides are predicted to have a metallic type of conductivity, as no energy gap was observed at or near the Fermi level (Fig. 6) and in a good agreement with experimental data. Localized DOS maximum in the range -8 ÷ -10 eV corresponds to the Sn *s*-states. Strong peaks near -4 eV belong to Cu *d*-states, while DOS above the Fermi level mainly corresponds to Hf *d*-states.

To evaluate similarities and differences in chemical bonding of ternary stannides in Hf-Cu-Sn system the distribution of the electron localization function (*elf*) was calculated (Fig. 7). In $HfCu_5Sn_2$ *elf* is mainly concentrated between pairs of Cu atoms and between Cu and Sn atoms. Almost spherical *elf* distribution around Hf atoms reflects some ionic nature of the formed compound. Similar situation is also observed in HfCuSn where the in-plane Cu-Sn hexagonal nets are connected via the Cu-Sn bonds, while Hf atoms play the same role as in the previous case. The last compound Hf_5CuSn_3 has significant differences as there are no direct Cu-Sn bonds, and each Cu atom is surrounded by Hf atoms. Main bonding is between Hf and Sn atoms, while Cu atoms are connected through $CuHf_6$ columns.

The calculated elastic constants of $HfCu_5Sn_2$, HfCuSn, and Hf_5CuSn_3 compounds show close values (Table 5). $HfCu_5Sn_2$ and HfCuSn exhibit larger C_{11} values in comparison to C_{33} which corresponds to the higher incompressibility along the *x*-axis, while Hf_5CuSn_3 shows higher C_{33} value. This difference between C_{11} and C_{33} causes higher anisotropy in $HfCu_5Sn_2$ and Hf_5CuSn_3 in comparison to HfCuSn. To estimate ductile and brittle

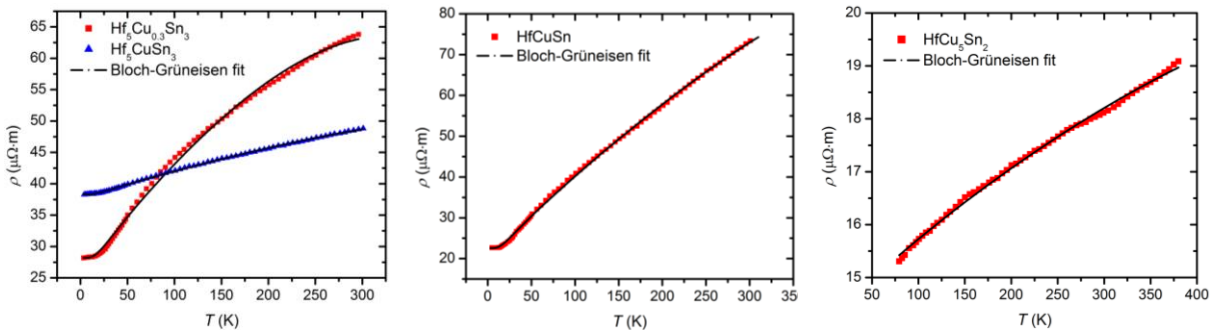

a *b* *c*

Fig. 5. Temperature dependence of electrical resistivity of the $Hf_5Cu_{0.3}Sn_3$, Hf_5CuSn_3, HfCuSn and $HfCu_5Sn_2$.

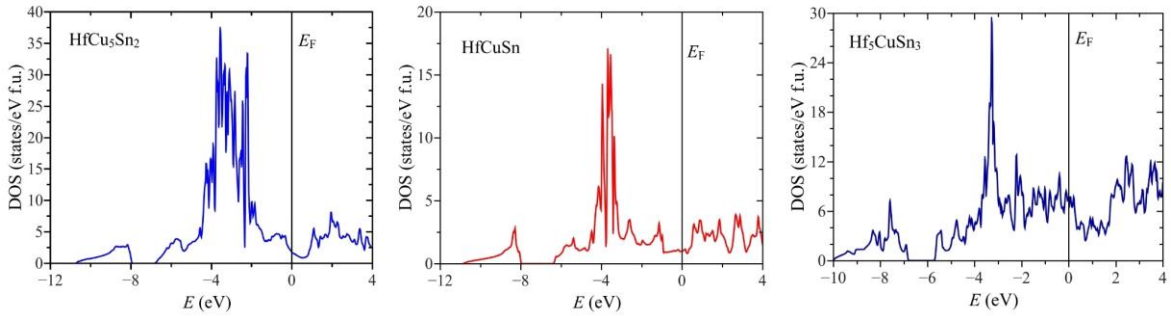

Fig. 6. Distribution of the total densities of states in $HfCu_5Sn_2$, HfCuSn, and Hf_5CuSn_3 compounds.

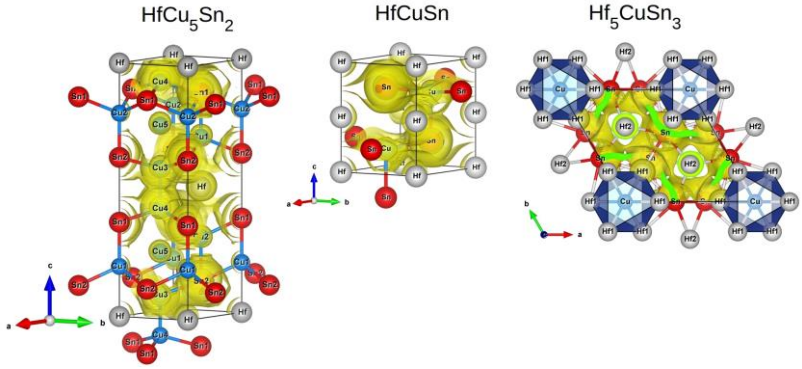

Fig. 7. Isosurface of the electron localization function at 0.33 in $HfCu_5Sn_2$, HfCuSn, and Hf_5CuSn_3 compounds.

behavior of investigated compounds the *B*/*G* ratio was calculated. For all stannides *B*/*G* > 1.75, and according to the Pugh [21] rule they should exhibit soft behavior and have low levels of hardness.

Final remarks

The performed investigations show that interaction of hafnium and tin with copper results in formation of three ternary phases at 870 K. Among them the Hf_5CuSn_3 compound corresponds to limited composition of the interstitial-type solid solution $Hf_5Cu_xSn_3$ (x = 0.0 - 1.0) based on Hf_5Sn_3 binary. The $HfCu_5Sn_2$ compound is typical only for the Hf-Cu-Sn system. Comparing the studied Hf-Cu-Sn system and taking into account the literature data for the related systems we may note that the ternary compounds of equiatomic composition appear in all the systems with Ti, Zr, Hf, copper and tin. The TiCuSn and HfCuSn compounds crystallize in the LiGaGe-type, while ZrCuSn stannide is characterized by orthorhombic TiNiSi structure type.

Romaka L. - Ph.D., Senior Scientist;
Romaka V. - D.Sc., Doctor of material science;
Stadnyk Yu. - Ph.D., Senior Scientist;
Horyn A. - Ph.D., Senior Scientist.

[1] M. Uysal, T. Cetinkaya, M. Kartal, A. Alp, H. Akbulut, *Production of Sn-Cu/MWCNT composite electrodes for Li-ion batteries by using electroless tin coating*, Thin Solid Films, 572, 216 (2014); https://doi.org/10.1016/j.tsf.2014.08.019.

[2] N. Jeong, E. Jwa, C. Kim, J.Y. Choi, J. Nam, S. Park, M. Jang, *Direct synthesis of carbon nanotubes using Cu-Sn catalyst on Cu substrates and their corrosion behavior in 0.6 M NaCl solution*, Appl. Surface Sci., 423, 283 (2017); https://doi.org/10.1016/j.apsusc.2017.06.021.

[3] B. Zhang, Y.G. Chen, H.B. Guo, *Effects of annealing on structures and properties of Cu-Hf-Al amorphous thin films*, J. Alloys Compd. 582, 496 (2014); https://doi.org/10.1016/j.jallcom.2013.07.190.
[4] Yu.V. Stadnyk, L.P. Romaka, *Phase equilibria in the Hf-Ni-Sn ternary system and crystal structure of the Hf_2Ni_2Sn compound*, J. Alloys Compd. 316, 169 (2001); https://doi.org/10.1016/S0925-8388(00)01036-7.
[5] L. Romaka, Yu.V. Stadnyk, O.I. Bodak, *Ternary Hf-Co-Sn system*, J. Alloys Compd. 317-318, 347 (2001); https://doi.org/10.1016/S0925-8388(00)01428-6.
[6] N. Melnychenko-Koblyuk, V.V. Romaka, L. Romaka, Yu. Stadnyk, *Interaction between the components in the {Zr, Hf}-Ag-Sn ternary systems*, Chem. Met. Alloys, 4, 234 (2011); https://doi.org/10.30970/cma4.0197.
[7] R.V. Skolozdra, L.P. Romaka, L.G. Alselrud, G.A. Melnik, Ya.T. Tatomir, *New phases of MgAgAs, LiGaGe and TiNiSi structural types containing d- and p-elements*, Neorg. Mater. 35(4), 1 (1999).
[8] J.C. Shuster, M. Naka, T. Shibayanagi, *Crystal structure of $CuSn_3Ti_5$ and related phases*, J. Alloys Compd. 305, L1 (2000); https://doi.org/10.1016/S0925-8388(00)00737-4.
[9] T.B. Massalski, Binary Alloy Diagrams, ASM, Metals Park, OH, (USA, 1990).
[10] S. Fürtauer, D. Li, D. Cupid, H. Frandorfer, *The Cu-Sn phase diagram, Part I: New experimental results*, Intermetallics, 34, 142 (2013); https://doi.org/10.1016/j.intermet.2012.10.004.
[11] J. Rodriguez-Carvajal. *Recent developments of the program FullProf. Commission on Powder Diffraction.* IUCr Newsletter, 26, 12 (2001); http://www.iucr.org/iucr-top/comm/cpd/Newsletters/.
[12] Elk, Program package; http://elk.sourceforge.net/.
[13] J.P. Perdew, K. Burke, M. Ernzerhof, *Generalized gradient approximation made simple*, Phys. Rev. Lett., 77, 3865 (1996); https://doi.org/10.1103/PhysRevLett.77.3865.
[14] K. Momma, F. Izumi. *"VESTA 3 for three-dimensional visualization of crystal, volumetric and morphology data"*, J. Appl. Crystallogr., 44, 1272 (2011); https://doi.org/10.1107/S0021889811038970.
[15] A. Gulans, S. Kontur, C. Meisenbichler, D. Nabok, P. Pavone, S. Rigamonti, S. Sagmeister, U. Werner, C. Draxl, *Exciting–a full-potential all-electron package implementing density-functional theory and many-body perturbation theory*, J. Phys.: Condens. Matter, 26, 363202 (2014); https://doi.org/10.1088/0953-8984/26/36/363202.
[16] R. Golesorkhtabar, P. Pavone, J. Spitaler, P. Puschnig, C. Draxl, *ElaStic: A tool for calculating second-order elastic constants from first principles*, Comp. Phys. Commun., 184, 1861 (2013); https://doi.org/10.1016/j.cpc.2013.03.010.
[17] J.P. Perdew, A. Ruzsinszky, G.I. Csonka, O.A. Vydrov, G.E. Scuseria, L.A. Constantin, X. Zhou, K. Burke, *Restoring the Density-Gradient Expansion for Exchange in Solids and Surfaces*, Phys. Rev. Lett. 100, 136406 (2008); https://doi.org/10.1103/PhysRevLett.100.136406.
[18] N. Melnychenko-Koblyuk, L. Romaka, L. Akselrud, V.V. Romaka, Yu. Stadnyk, *Interaction between components in Hf-Cu-Sb ternary system at 770 K*, J. Alloys Compd., 461, 147 (2008); https://doi.org/10.1016/j.jallcom.2007.07.012.
[19] E.I. Gladyshevskii, O.I. Bodak, V.I. Yarovets, Y.K. Gorelenko, R.V. Skolozdra, *Studies in crystalline structure and magnetic susceptibility of the $R_2Fe_4Si_9$ and $RFeSi_3$ (R=Y, Gd, Tb, Dy, Ho, Er, Tm, Yb, Lu) compounds*, Ukr. Fiz. Zh. 23, 77 (1978).
[20] G.V. Samsonov, Mechanical Properties of the Elements Handbook of the physicochemical properties of the elements, (New York, USA, 1968).
[21] S.F. Pugh. *Relations between the elastic moduli and the plastic properties of polycrystalline pure metals*, Philos. Mag. A, 45, 823 (1954); https://doi.org/10.1080/14786440808520496.

Л. Ромака[1], В.В. Ромака[2], Ю. Стадник[1], А. Горинь[1]

Експериментальне дослідження потрійної системи Hf-Cu-Sn при 870 K

[1]*Львівський національний університет ім. І.Франка, м. Львів, Україна, lyubov.romaka@gmail.com*
[2]*Інститут дослідження твердого тіла ім. Лейбніца, Дрезден, Німеччина, v.romaka@ifw-dresden.de*

Взаємодію гафнію з купрумом і станумом досліджено при 870 K у повному інтервалі концентрацій методами рентгенівського аналізу і скануючої електронної мікроскопії. За температури дослідження в системі Hf-Cu-Sn утворюються три тернарні сполуки: HfCuSn (стр. тип LiGaGe), $HfCu_5Sn_2$ (стр. тип $HfCu_5Sn_2$) і Hf_5CuSn_3 (стр. тип Hf_5CuSn_3). Нова тернарна сполука $HfCu_5Sn_2$ кристалізується в просторовій групі $P6_3/mmc$ з періодами гратки a = 0,42959(7) нм, c = 1,54165(4) нм. Електротранспортні властивості засвідчують металічний тип провідності для всіх досліджених тернарних сполук. Розрахунки DFT використані для оцінки хімічного зв'язку, еластичних і фізичних властивостей тернарних фаз.

Ключові слова: інтерметаліди; фазові діаграми; рентгенівська дифракція; кристалічна структура; електричні властивості.